Dispersive Properties of Optical Filters for WDM Systems

G. Lenz, B. J. Eggleton, C. R. Giles, C. K. Madsen, and R. E. Slusher

***Abstract*— Wavelength division multiplexing (WDM) communication systems invariably require good optical filters meeting stringent requirements on their amplitude response, the ideal being a perfectly rectangular filter. To achieve high bandwidth utilization, the phase response of these filters is of equal importance, with the ideal filter having perfectly linear phase and therefore constant time delay and no dispersion. This aspect of optical filters for WDM systems has not received much attention until very recently. It is the objective of this paper to consider the phase response and resulting dispersion of optical filters in general and their impact on WDM system performance. To this end we use general concepts from linear systems, in particular, minimum and nonminimum phase response and the applicability of Hilbert transforms (also known as Kramers–Krönig relations). We analyze three different classes of optical filters, which are currently being used in WDM systems and compare their performance in terms of their phase response. Finally, we consider possible ways of linearizing the phase response without affecting the amplitude response, in an attempt to approximate the ideal filter and achieve the highest bandwidth utilization.**

***Index Terms*—Dispersive channels, gratings, waveguide filters, wavelength division multiplexing.**

I. Introduction

WAVELENGTH division multiplexing (WDM) is becoming pervasive in optical communication systems. Key optical components in these systems are those that perform the function of combining (multiplexing) different wavelength channels and splitting (demultiplexing) them. Combining different wavelengths is a relatively simple task and can be achieved with a component such as a star coupler. Demultiplexing requires optical spectral filters and is a much more challenging problem when real system constraints are applied.

In recent years, a number of candidates for this filtering function have been proposed and implemented and can be divided broadly into three categories: 1) Mach–Zehnder interferometer (MZI) based devices which include the waveguide grating router (WGR) [1] and the Fourier filters [2]; 2) thin-film filters (TFF's) which include multiple cavity transmission filters [3], Fabry–Perot filters, and ring resonator filters [4]; and 3) fiber Bragg gratings (FBG's), including apodized [5] and chirped gratings [6]. We will designate these as class I, II, and III filters, respectively. Another filter type that is used in WDM systems is an absorption filter for frequency standards and frequency stabilization. These filters are usually materials with a very narrow absorption line (see, e.g., [7] where an acetylene molecular line is used). We will not discuss absorption filters further in this paper, since their dispersive properties are well understood and obey the Kramers–Krönig relations.

The amplitude response is usually constrained by system considerations in a number of ways: 1) insertion loss—total loss in the passband of the filter; 2) crosstalk—rejection of out-of-band signals; 3) sharpness—"steepness" of the filter edges; and 4) spectral structure both in the passband (e.g., ripple and flatness) and outside the passband (e.g., side lobes). Of equal importance is the phase response of a filter which is responsible for total time delay through the filter (first derivative of the spectral phase) and dispersion-induced pulse distortion (second and higher derivatives of the spectral phase response). While the amplitude response of the above filters is well understood and has received much attention, the phase response has only recently been investigated in the context of communication systems [8], [9].

While dispersion effects and dispersion compensation in optical fiber systems has been an active area of research (see e.g., [10]), the dispersion associated with the filtering elements in the system have not been studied in detail. The purpose of this paper is to clarify the consequences of the phase response of optical filters, compare their performance in terms of their dispersive properties, and consider the impact of their dispersion on WDM systems. Many of these issues have been explored and explained in the field of electrical engineering, in particular in areas such as electrical circuit theory and digital signal processing, and we shall make use of some of this body of knowledge and apply it to optical filters. Some work has been done in this area previously (see, e.g., [11]), however, there has not been a systematic study and explanation of the dispersive properties of different optical filters.

To understand the impact of these dispersive properties, we may think of a single channel carrying information at a given bit rate passing through a dispersive filter. The dispersion induces broadening and distortion of the bits, which ultimately lead to transmission errors (for a detailed discussion of these effects when the filter is an apodized fiber grating, see [8]). Ideally, we would like a filter having a rectangular amplitude response and zero dispersion (which corresponds to linear spectral phase over the filter's passband), i.e., a spectral response of the form

$$H(\omega) = \begin{cases} e^{-j\omega T}, & |\omega| < \omega_c \\ 0, & \text{otherwise} \end{cases} \quad (1)$$

Manuscript received January 9, 1998; revised April 16, 1998.

G. Lenz, B. J. Eggleton, C. K. Madsen, and R. E. Slusher are with Bell Laboratories, Lucent Technologies, Murray Hill, NJ 07974 USA.

C. R. Giles is with Bell Laboratories, Lucent Technologies, Holmdel, NJ 07733 USA.

Publisher Item Identifier S 0018-9197(98)05419-0.

where $H(\omega)$ is the complex frequency response (complex transmission), ω_c is the cutoff frequency (the bandwidth of the filter is $2\omega_c$), and T is the group delay through the filter. Note, also, that we treat here a low-pass filter rather than a bandpass filter centered at the optical frequency. This type of filter would let us pack the different wavelength channels as close as possible without crosstalk or dispersion penalties leading to a spectral efficiency or bandwidth utilization of 1 bit/s/Hz (i.e., channel bit rate = channel spacing) without any special coding scheme. It can be shown (by direct Fourier transformation), however, that this type of filter is a noncausal filter (which can have an output *before* an input is applied). We would therefore like to approximate such an ideal filter as closely as possible.

The paper is structured as follows. In Section II, we will discuss the concept of minimum phase filters (MPF's) and nonminimum phase filters. For MPF's there is a unique relationship between the amplitude response and the phase response. If the amplitude response is known or measured for such a filter, the phase response can be derived using a linear transformation known as the Hilbert transform (which is related to the well-known Kramers–Krönig relations in optical physics). Section III will compare the phase response of the three different classes of optical filters introduced earlier and consider the consequences of the associated dispersion for WDM systems. In Section IV, we will discuss ways of designing low dispersion and dispersionless filters by using non-MPF's (which is also a well-known technique used by electrical engineers in analog and digital filter design) and the feasibility of such filters. Section V will offer our conclusions. Appendixes A–D contain a number of mathematical appendices relevant to the discussions in this paper.

II. Minimum Phase Filters

In this section we will introduce the important concept of minimum phase systems where the phase response is uniquely determined by the amplitude response. We will discuss in some detail the properties of such systems and point out the important differences between them and nonminimum phase systems. This formalism will then be applied to optical filters. In Section II-A we introduce the notation and terms of linear systems (analog and digital). Section II-B is a more technical discussion of the properties of minimum phase systems. Finally, in Section II-C, we discuss optical filters in the context of minimum phase and nonminimum phase linear systems.

A. Hilbert Transforms in Linear Systems

Filters are linear systems which are completely characterized by their impulse response function $h(t)$. The system function is the Laplace transform of $h(t)$ and is a function of the complex variable s also known as the complex frequency. The frequency response $H(\omega) = |H(\omega)| \exp(j\phi(\omega))$ is derived by evaluating $H(s)$ on the imaginary axis in the complex s plane, i.e., setting $s = j\omega$ in $H(s)$. An alternative representation used in digital filter theory has $h(n)$ as the discrete impulse response function defined at times nT and a corresponding system function $H(z)$ which is the z transform of $h(n)$. There is a simple bilinear transformation (or conformal mapping) given by

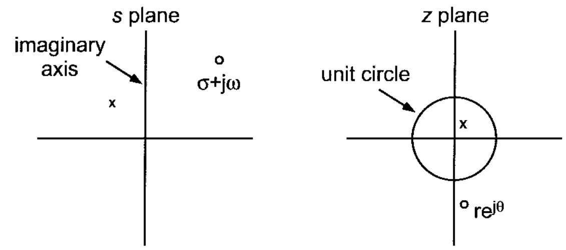

Fig. 1. Schematic of the complex s plane (using rectangular coordinates) commonly used analog filter design and the complex z plane (using polar coordinates) commonly used in digital filter design. There is a conformal mapping between these two planes, which has been used to show the equivalent locations of a pole (marked with an $\times$) and a zero (marked with an $\circ$).

$$z = \frac{1 + (T/2)s}{1 - (T/2)s} \tag{2}$$

that maps the s plane onto the z plane: the right half of the s plane maps onto the outside of the unit circle, the left half of the s plane maps onto the inside of the unit circle and the imaginary axis in the s plane maps onto the unit circle in the z plane. To get the frequency response, $H(z)$ is evaluated on the unit circle, i.e., setting $z = e^{j\omega}$. To clarify these concepts, Fig. 1 shows a schematic of both the s plane and the z plane. In the following discussions it will be understood that anything said about $H(s)$ and $H(\omega)$ applies to $H(z)$ and $H(e^{j\omega})$ with the above mapping. Note also that we will adhere to the conventions of digital filters where ω is the frequency normalized to the unit delay T.

For a linear system to be causal, there is an added constraint, namely $h(t) = 0$ for $t < 0$, and for the system to be stable the "area" under $|h(t)|$ must be finite (we will consider only passive systems containing no gain). It is well known that causality implies dispersion [12], [13] and that there is a unique relation between the real and imaginary parts of the frequency response. This relation is known as a Hilbert transform and can be applied to the real part of the frequency response to get the imaginary part, *if* the corresponding $h(t)$ is real, stable, and causal. It would seem that if we take the natural logarithm of $H(\omega) = |H(\omega)| \exp(j\phi(\omega))$ we would be able to apply the Hilbert transform to $\ln|H(\omega)|$ to get $\phi(\omega)$ and that this relation would also be *unique*. However, for this to be true, $\hat{h}(t)$, the inverse Fourier transform of $\ln(H(\omega))$, must be real, stable, and causal. If this is the case the system is said to be minimum phase (for reasons that will be explained later). Bode was the first to point out the minimum phase condition. He also showed that systems meeting this condition are a subclass of all linear systems for which Hilbert transforms may be used [14].

Note that $h(t)$ may be causal while $\hat{h}(t)$ is noncausal, in which case the system is said to be nonminimum phase and the Hilbert transform may *not* be applied. In areas such as optical physics where the Kramers–Krönig relations (an equivalent form of the Hilbert transform) are used between absorption (amplitude response—$|H(\omega)|$) and refractive index (phase response—$\phi(\omega)$), the frequency response is always of the minimum phase type. In fact, material dispersion is fundamentally different than geometrically induced or structurally induced dispersion, which we are considering in this paper. Adjustable geometrically induced dispersion can be found in many optics applications such as waveguide dispersion in fibers [15] and the so-called zero dispersion compressor [16], commonly used in the field of femtosecond optics. Material dispersion comes from absorption resonances (even in a *single* atom) and so terms like reflection, for example, are meaningless in this context but are very important in the context of some of the non-MPF's that we will discuss. For an alternative discussion of non-MP systems and Kramers–Krönig relations, see [17].

B. Properties of MPF's

Having defined MPF's, we now look at some of their properties.

1) MPF's are filters for which $H(s) \neq 0$ for all $s > 0$, i.e., which have no *zeros* in the right-half plane. Filters that have zeros only on the imaginary axis (i.e., real zeros in the frequency response) are a special case and will be discussed later.
2) It can be shown that any MPF can be followed by an arbitrary number of different all-pass filters, which do not affect the amplitude response but do modify the phase response. This is common practice in electronic filter design, when phase linearization is required. An all-pass filter is defined as one having zeros in the right-half plane and corresponding poles symmetrically around the imaginary axis in the left-half plane. It is easily shown that such filters have a pure phase response. This can be shown with the help of equation (D2) in the appendix dealing with all-pass filters: by taking the magnitude of that expression we get a frequency independent amplitude α with a frequency dependent phase (the issue of finite bandwidth in real optical filters will be addressed later).
3) The infinite number of non-MPF's derived from a MPF (by following it with any combination of all-pass filters) have *greater* phase lag than the original MPF at *any* point in frequency as well as *greater* time delay (defined as $\tau = -d\phi/d\omega$). In other words, MPF's are not only minimum phase but also minimum delay.
4) For MPF's the difference between the phase at zero frequency and infinite frequency is smaller than that of any non-MPF derived from it. This, in conjunction with the previous remark, means that the phase of a MPF is constrained to the narrowest range in phase.
5) The inverse of a MPF (i.e., $1/H(s)$) is also a MPF (non-MPF's, having zeros in the right-half plane, will give right-half plane poles when inverted and lead to an unstable system).

The great advantage of non-MPF's is that the phase response may be adjusted without changing the amplitude characteristics, in particular, the phase may be linearized to give constant delay and therefore no dispersion.

The problem of filters with zeros *only on* the imaginary axis is an important one, since many optical filters of interest have zeros in their frequency response ($|H(\omega)| = 0$ for some ω). Strictly speaking, these are non-MPF's as can be seen by looking at the inverse of these filters. However, it has been pointed out that in some limited sense these should also be considered MPF's (see discussion in [18]). It should also be noted that adding an infinitesimal amount of loss will shift these zeros to the left-half plane, making them MPF's to which the Hilbert transform may now be applied. To avoid this problem altogether, we will just add a very small loss to these types of filters and treat them as MPF's. Once a filter is identified as a MPF to which Hilbert transforms may be applied, some very general statements may be made about the relationship between the amplitude and phase response. This will help us in the comparison of different optical filters.

C. Optical Filters

For the case of *optical* filters, a few more comments have to be made about the finite bandwidth and the material dispersion. We will assume that the *material* dispersion is negligible, which is equivalent to the statement that the *material* absorption is flat over a very large bandwidth (this is usually true in the transparent regions far from any absorption peaks). In other words, we will be mainly interested in the dispersion and amplitude response associated with the filter itself (i.e., the structurally induced dispersion defined earlier) and ignore the small corrections arising from the spectral response of the material. Note also that in WDM systems the required filters have a typical bandwidth of the order of 1 nm. Even over the whole system bandwidth, constrained currently by the 80-nm bandwidth of erbium-doped fiber amplifiers [19], the spectral response of the material is essentially constant.

All of the optical filters we will consider may be modeled as digital filters and the exact frequency response of the filters can be derived from $H(z)$ evaluated at $z = e^{j\omega}$. In linear systems theory, in some cases, $h(n)$ is a sampled version of a continuous $h(t)$ (evaluated at $t = nT$)—this is not the case here. Therefore, we do not need to worry about going back to the continuous $h(t)$, satisfying the sampling theorem, etc. [20]. In the following discussions on optical filter we will restrict ourselves to discrete systems.

To make this discussion more concrete we show a simple optical filter, which is a non-MPF. The filter consists of a thin dielectric film of refractive index n_2 and thickness d, sandwiched between two semi-infinite media of refractive indices n_1 and n_3 with $n_2 > n_3 > n_1$. We will look at the complex reflection coefficient when reflecting off one side as compared to reflecting off the opposite side. As will be shown, the amplitude response is identical, yet the phase response is very different. When the incident light is coming from the n_1 side, the complex reflection may be written as follows:

$$r = \frac{(q-p)\cos\delta - i(1-qp)\sin\delta}{(q+p)\cos\delta + i(1+qp)\sin\delta} \tag{3}$$

where $q = n_1/n_2, p = n_3/n_2$, and $\delta = (2\pi/\lambda)n_2 d$. When the light is incident from the n_3 side, q and p are interchanged.

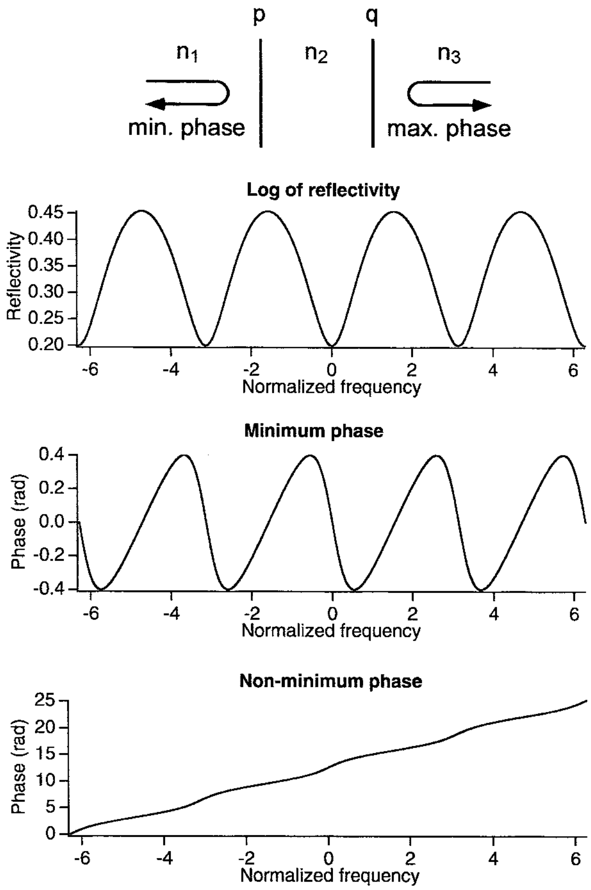

Fig. 2. Example of a nonminimum phase optical filter. The filter consists of a thin film with refractive index n_2 surrounded by two semi-infinite media with refractive index n_3 and n_1 such that $q = 0.5$ and $p = 0.75$ in (3). The amplitude response is the same regardless of the input direction, however, the phase of the reflection depends on the input side—from the low index side the phase response corresponds to the minimum phase response, but from the high index side the phase response is nonminimum phase (and is shown to be the maximum phase response).

Examining the above relation it is clear that only the phase will change upon an interchange of q and p. Fig. 2 shows the amplitude response (which is the same from both sides) and the phase response of the reflection from the two different sides. It can be shown by applying the Hilbert transform to $\ln|r(\omega)|$ that the resulting phase response is identical to the one derived from (3) when incident from the lower index side, n_3. This means that from the lower index side we get the minimum phase response and from the higher index side we get a nonminimum phase reflection response (which will later be shown to be the so-called maximum phase response). Other examples of nonminimum phase response of optical filters are given in [11], notably the Gires–Tournois interferometer, for which the system function contains zeros in the right-half s plane (since it is a purely reflective filter by design [21], it is a special case of class III rather than class II filters). In the following section, we will discuss why non-MPF response can be found *only* in reflection responses of class II and III filters, but not in their transmission response.

A final very useful result that applies exclusively to MPF's relates the derivative of the amplitude response to the phase response. This result may be written as follows [14]:

$$B(\omega_c) = \frac{1}{\pi}\int_{-\infty}^{\infty} \frac{dA}{du} \ln\coth\frac{|u|}{2}\, du \tag{4}$$

where $u = \ln(\omega/\omega_c)$ is a normalized frequency and A and B are a Hilbert transform pair—real and imaginary part or logarithm of magnitude and phase. This may be understood as follows: the phase at frequency ω_c depends on the slope of the amplitude response at all points of the spectrum weighted by the factor $\ln\coth|u/2| = \ln|(\omega+\omega_c)/(\omega-\omega_c)|$. This weighting factor is strongly peaked at $u = 0$ ($\omega = \omega_c$) and is equal to $2(\omega_c/\omega)$ and $2(\omega/\omega_c)$ for frequencies far above and below ω_c, respectively. A number of conclusions may be drawn from this relation: 1) features in the amplitude response which are "far away" from ω_c do not contribute much to the phase response at this frequency; 2) the above relation also implies that a constant amplitude response implies linear phase; and 3) since u corresponds to a logarithmic frequency scale, we can plot the amplitude response on such a scale and examine its derivative in the vicinity of the frequency where we want to evaluate the phase. Over a narrow spectral range the weighting factor can be taken to be approximately constant so that the weighting function may be taken out of the integral. The phase is then directly related to the *change* in the amplitude response.

The last point is of great importance since it relates the slope of the amplitude response to the phase response. When the amplitude response changes radically (e.g., near the passband edges), the phase will change correspondingly going from the approximately linear phase to one containing higher order terms leading to dispersion. The result is that as the ideal amplitude characteristic is approached, the dispersion increases near the band edges. This is illustrated in Fig. 3 for the ideal rectangular filter showing a phase characteristic, which is highly nonlinear as the passband edges are approached, ultimately diverging at the band edges. Again, since this result holds *only* for MPF's, using non-MPF's avoids this phase behavior.

III. WDM Filter Comparison

In the introduction we have identified three broad classes of WDM filters currently in use or under consideration. Class I filters are transmission filters in which inherently there is no light lost to reflection. Class I filters are also very similar to electronic digital finite impulse response (FIR) filters [20]; this statement and its implications will be discussed in greater detail later. Note also that these are parallel devices—to demultiplex many wavelengths does *not* require many devices in series.

Class II filters are in general transmission filters and are also known as interference filters. To create an N-channel WDM component, many of these individual filters have to be cascaded serially and in this case the wavelength that is transmitted through the last filter in the series has undergone $N-1$ reflections off the previous filters. These multiple reflections will be significant when the neighboring channel dispersion is considered.

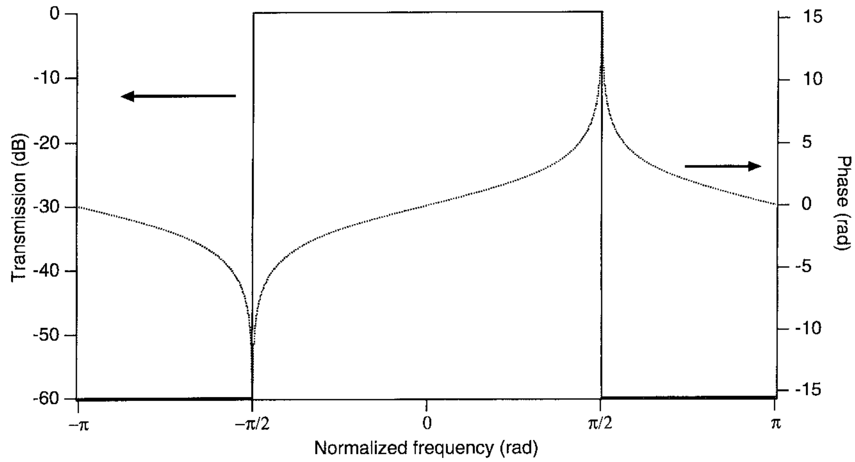

Fig. 3. Phase response (dotted line) of the ideal rectangular filter (solid line) assuming the filter is a MPF, so that this phase response may be calculated by applying the Hilbert transform to the logarithm of the magnitude of the amplitude response. As the edges of the passband are approached, the phase becomes nonlinear and diverges at the edges.

Class III filters are in some sense similar to class II filters in that their operation is based on interference effects from multiple "layers." Class III filters are typically reflective filters and the achievable refractive index contrast ratio of a grating is much smaller than the one possible with dielectric stacks used in class II filters. Here, as in class II filters, the dispersive effects of the filter on neighboring channels are significant, especially when many individual devices are cascaded in a serial manner.

A. Class I Filters (WGR- and MZI-Based Filters)

We now turn to a more detailed analysis of these filter classes specifically looking at the dispersion effects on the filtered channel as well as the effects on the neighboring channels. We first consider class I filters and in particular look at the WGR as a representative of this class. Essentially, the response of this device is a sum of a finite number of weighted fixed delays and may be written as

$$H(\omega) = \sum_{n=0}^{N-1} h(n) e^{-j\omega n} \tag{5}$$

where $h(n)$ is the discrete impulse response, N is the number of WGR arms, and ω is the normalized frequency. This type of response is well known in digital filters and the corresponding filter is called a finite impulse response (FIR) filter. From this expression we can also immediately see that the response is periodic since replacing ω by $\omega + 2\pi k$ (k integer) will not change the response. For this type of filter it can be shown (see Appendix A) that if $h(n) = h(N-1-n)$ then the filter has *exactly* linear phase. In this case the filter is non-MPF since $H(z)$ has zeros which are not inside the unit circle. When the only zeros are *on* the unit circle, as in standard WGR's, a small realistic loss may be introduced with the effect of shifting the zeros inside the unit circle, thereby making the filter a MPF. This results in only very small dispersion (i.e., departure from phase linearity) at the very edges of the filter passband. This is demonstrated in Fig. 4 for the case where $h(n) = 1$ for $0 < n < N-1$. Using (5), the response is given by

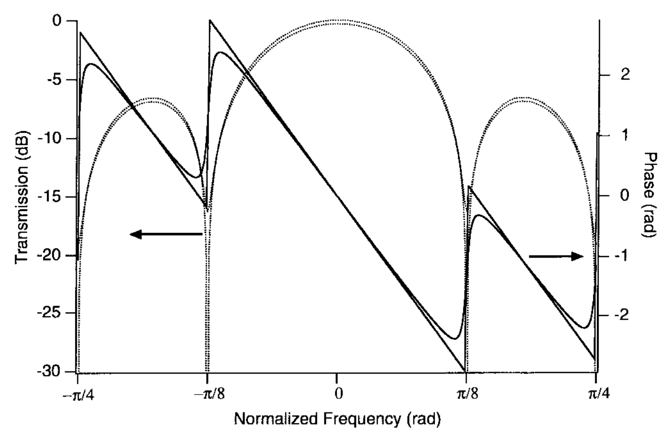

Fig. 4. The effects of adding loss to the simple WGR. The dotted line compares the amplitude response with and without loss and the solid line the compares the phase response. Equation (5) was used with $N = 16, h(n) = 1$, and ω was replaced by $\omega - j0.01$ to illustrate the effects of loss. This implies a relative transmission loss between the WGR arms of ~1% which is unrealistically large. Typically the phase response departs from linearity when the transmission is down 20 dB or more.

$$\begin{aligned} H(\omega) &= \frac{1 - \exp(-j\omega N)}{1 - \exp(-j\omega)} \\ &= \exp(-j\omega(N-1)/2) \frac{\sin(N\omega/2)}{\sin(\omega/2)}. \end{aligned} \tag{6}$$

As expected for real ω, the phase is linear. The loss was introduced by adding a small constant imaginary part to the frequency ω. It is interesting to note that an N-stage cascaded MZI with delays doubling in successive stages has exactly the same response as a 2^N-arm WGR (see [21], which treats birefringent Lyot–Ohman filters that are equivalent to cascaded MZI's). For this WGR example, we have used a square weighting function or window, i.e., all the arms are illuminated with the same intensity. A more realistic window function is a Gaussian distribution since it is the natural result of the light diffracting in the first free-space coupler region of the router before entering the fixed delay waveguides. For large N, the

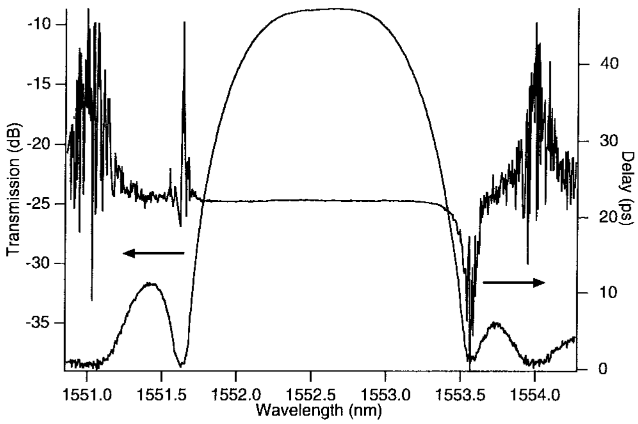

Fig. 5. The measured transmission spectrum and group delay of a WGR with flattened passband. As can be seen, the group delay is constant (zero dispersion) over most of the passband. Dispersion sets in at the points where the transmission is about 20 dB down from the peak. This dispersion is attributed to various loss mechanisms, which constitute a departure from the ideal dispersionless behavior of these devices.

$h(n)$ may be taken as a binomial distribution to approximate a Gaussian distribution for which the response is

$$\sum_{n=0}^{N-1} \binom{N-1}{n} e^{-j\omega n} = (1+e^{-j\omega})^{N-1} = 2^{N-1} \exp\left(-j\omega(N-1)/2\right) \cdot \cos^{N-1}(\omega/2). \quad (7)$$

Here again the phase is linear because of the symmetry of the binomial distribution. This demonstrates that even for the more realistic models of the WGR the phase is still inherently linear and the device is practically dispersionless. The small dispersion that is typically found in the measurement of these devices is attributed to residual losses in the waveguides, coupling efficiencies into the output waveguides, etc. Fig. 5 shows the results of such a measurement in a device which was also designed to achieve flatter passbands, however, this did not change the inherent linear phase characteristic as is evident from the very constant delay over most of the passband.

Finally, since class I filters are essentially FIR digital filters, digital signal processing (DSP) techniques may be applied to these filters to improve their amplitude characteristics without affecting the linear phase property. This will be discussed further in the next section.

B. Class II Filters (Interference Type Filters)

We now turn to class II filters and in particular we will consider the multiple cavity TFF's [3]. These filters are made of dielectric layers with a very high refractive index contrast (typically $\Delta n \sim 1$). A quarter-wave stack with a quarter-wave shift in its center creates a resonant transmission in the stopband of the stack and because of the high index ratio this may be accomplished with a relatively small number of layers. By growing a number of such cavities (typically 3–5) on top of each other, this transmission peak may be "squared" but at the expense of added ripple in the passband, which gets worse with increasing number of cavities. Another consequence of the

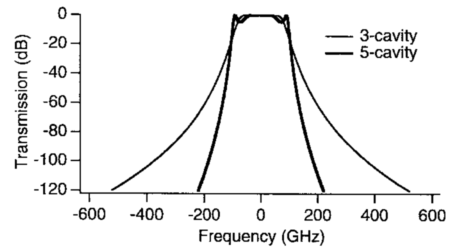

(a)

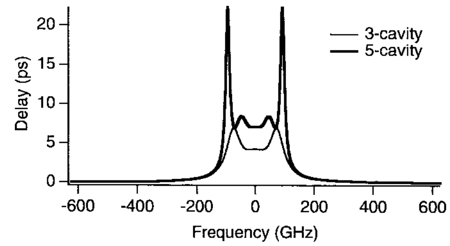

(b)

Fig. 6. (a) The transmission spectrum and (b) group delay of a TFF with three cavities (thin line) and five cavities (thick line). Each cavity contains two quarter-wave stacks spaced by one half-wave layer, and each stack contains seven periods with refractive indices $n_1 = 1.445$ and $n_2 = 2.4$. Increasing the number of cavities gives a squarer transmission but comes at a price of ripple in the passband and higher dispersion near the passband edges.

high index ratio is a very large stopband (fractional bandwidth $\Delta\omega/\omega$ of about 1/3), however, the transmission peak width is on the order of 1 nm, which means we can analyze the transmission peak alone, ignoring the small dispersion contributions from the distant stopband edges. It has been shown that for a general thin film filter with arbitrary layer structure the *transmission* response is an all pole response, i.e., it has *no* zeros and therefore is by definition minimum phase [22] (see Appendix C). The simplest example is a symmetric Fabry–Perot filter, which has a complex amplitude transmission $t = T\exp(-i\phi)/(1-R\exp(-2i\phi))$ [20], where R and T are the reflectance and transmittance, respectively, and ϕ is the frequency-dependent phase accumulated in one trip through the filter. Obviously, there is *no* frequency (real or complex) for $R \neq 1$ that will result in a pole in t. Using matrix techniques as in [22] to get the exact transmission response, it can be easily verified that the multiple cavity filters in general have no zeros in their transmission response and are indeed MPF's. As explained earlier, this means that steepening the filter's edge by increasing the number of cavities will not only add ripple in the passband but also increase the dispersion near the edges [see (4)]. Fig. 6 shows the amplitude and phase response of a three- and five-cavity filter.

Although the transmission response of these filters is very important, we cannot ignore the reflection response, since for a demultiplexer one needs to cascade a number of these filters in series. This means that the phase response of the reflection may introduce dispersion in a neighboring channel. This may cause distortion in that channel and ultimately lead to errors. An analogous situation happens with FBG's where the neighboring *transmitted* channel may suffer a dispersion-induced penalty [8]. We will discuss this in more detail in the context of class III filters.

Finally, we make some general remarks about class II filters some of which will also apply to class III filters. As was shown in [22], any optical multilayer structure's reflection response may be written as a digital filter response of the form

$$H(z) = \frac{\sum_{k=1}^{N} b_k z^{-k}}{1 - \sum_{k=1}^{N} a_k z^{-k}} \tag{8}$$

where the a_k's and b_k's are constants derived from the reflection coefficients between the different layers and N is the total number of layers. The transmission response as discussed above will have only poles (at the same places as the reflection response) and no zeros, making it a minimum phase response. The response as written above assumes that all the layers have the same optical thickness, but can easily be generalized as shown in [22]. The frequency response [(8) with $z = e^{j\omega}$] is periodic for the same reason that class I filters are periodic.

To see the effects of a given system function on the phase response and the dispersion, we can look at how the structure of the system function affects the group delay of the filter (see Appendix B for a detailed discussion). The total group delay can be shown to be the sum of the delays due to the function's poles minus the function's zeros. It can also be shown that the major contributions to this delay come from poles and zeros located close to the unit circle and that the delay is peaked at frequencies close to the locations of those poles and zeros.

The response in (8) is known as an infinite impulse response (IIR) and inherently involves feedback [20], as one would expect, since multiple reflections are involved in these filters and reflection is inherently a feedback mechanism. This is where class II and III filters are markedly different than class I filters which were shown to be FIR filters. Note also that even though a class II or III filter may have all its zeros on the unit circle in the z plane (e.g., the case for uniform FBG's) as standard WGR's do, the poles, which are not present in the WGR, will "destroy" the phase linearity. It is because FIR filters have *only* zeros that they are naturally good candidates for linear phase filters.

Another way of looking at IIR filters is that because of their inherent feedback mechanism they can store energy; at some frequencies the photon lifetime becomes very large and consequently the group delay becomes very long as these frequencies are approached.

As can be seen, the function in (8) becomes very complex with an increasing number of layers N, and this is especially true for FBG's which may contain hundreds of thousands of effective layers and a corresponding number of zeros and poles. Correcting their phase response by designing a filter in cascade such that it would correct or linearize the phase may prove difficult.

Finally, we make some comments about the reflection response of Fabry–Perot filters and explain the results of the example in the previous section, which was an *asymmetric* Fabry–Perot filter. The simplest TFF is a Fabry–Perot filter consisting of a single thin film sandwiched between two *identical* semi-infinite media. Using (8) we see that the response function contains a single zero and a single pole. Since the single zero is at $z = 1$ the filter is a MPF in reflection. When the filter is asymmetric, i.e., a thin film sandwiched between two *different* media, the location of the zero depends on the input side. When reflecting off the low index side the zero is inside the unit circle at some z_1 and the response is minimum phase. When reflecting off the high index side the zero is outside the unit circle at $1/z_1^*$ (here the asterisk denotes complex conjugation) and the response is nonminimum phase and in fact is known as maximum phase (minimum phase has all the zeros inside the unit circle; similarly maximum phase has all its zeros outside the unit circle). As mentioned in the previous section, the amplitude response is the same regardless of input side and the Hilbert transform would yield the right answer only for one side (the minimum phase side).

In general, spatially asymmetric structures in reflection will be nonminimum phase at least from one side. If the response from one side has zeros both in and outside the unit circle, it will have the "mirror image" zeros when reflecting off the opposite side. The zeros that were inside will now be outside the unit circle and vice versa according to $z_i \to 1/z_i^*$. Following [22] we find that going from the reflection off one side to the reflection off the other side involves changing the sign of all the reflection coefficients and reversing the order of matrix multiplication. Since these matrices generally do not commute, it is easy to see why the reflection response in a spatially asymmetric structure would be different when reflecting off the two sides. Spatial symmetry, however, does not imply minimum phase as can be verified, e.g., in a symmetric three-layer filter where the central layer has higher index than the two identical neighboring layers and the whole filter is surrounded by air. The reflection response, which is obviously identical from both sides, is nonminimum phase, since one of its three zeros is outside the unit circle. However, as is shown in Appendix C for the case of a general symmetric structure, if a constant group delay corresponding to the optical length of the structure is subtracted from the total delay, the remainder is MP. In other words, given a spatially symmetric structure, the *dispersion* can be computed from the amplitude response, using the Hilbert transform and differentiating twice (since the constant delay contributes zero dispersion).

C. Class III Filters (FBG Type Filters)

Class III filters are very similar to class II filters in their properties and differ only in two ways: 1) class II filters operate in transmission and class III operate in reflection and 2) class II filters typically have a very high refractive index contrast between the different layers, whereas class III filters involve relatively small index modulation $(\Delta n/n \ll 1)$ and can therefore be modeled very well by the approximate coupled-mode theory. This also means that type II filters require only a small number of layers, but type III filters involve many "layers" and thus are longer devices. In spite of these differences, the formalism applied to class II filters is appropriate for class III filters and we expect some of the same conclusions to apply.

There has recently been growing interest in the phase response of FBG's mainly in the context of phase reconstruction from reflection data [23]–[25]. It was realized in these papers that the reflection response has to be minimum phase in order to be able to *uniquely* infer the phase from the amplitude response by means of a Hilbert transform. Using coupled mode theory, it was pointed out in [24] that asymmetric structures are inherently nonminimum phase, at least from one side, and that indeed the phase response will always be between the minimum and maximum phase response. This is especially important to realize when dealing with structures such as chirped gratings.

Using some of the results of the last section, we make some general comments about class III filters.

1) Since class II filters work in transmission, the filtered signal always sees a MPF. The dispersion of the transmitted signal may therefore be directly calculated from the transmission amplitude response using the Hilbert transform. This is not the case for class III filters, however, the dispersion of the neighboring *transmitted* channel may be determined uniquely.
2) When the response is minimum phase (e.g., in the case of a uniform grating), "squaring" the filter function by making a stronger grating will result in larger dispersion close to the edges because of the large derivative change in the amplitude response (as explained earlier).
3) When there is spatial asymmetry in the device, whether by design, processing imperfection, or processing error, the dispersion will depend on the input side.

To get a more quantitative view of FBG's, we will examine the dispersion of the reflected channel from a uniform grating using coupled mode theory. The reflection is given by [21]

$$r = \frac{-i\kappa \sinh(\alpha L)}{\alpha \cosh(\alpha L) + i\delta \sinh(\alpha L)}, \quad \alpha = \sqrt{\kappa^2 - \delta^2} \tag{9}$$

where κ is the coupling constant given by $\kappa = \pi \Delta n \eta / \lambda_B$, Δn is the refractive index modulation, η is the fraction of the energy in the fiber core, and λ_B is the Bragg wavelength. The detuning parameter is $\delta = (n/c)(\omega - \omega_B)$ where n is the average effective index, c is the speed of light, ω is the frequency and $\omega_B = 2\pi c/\lambda_B$ is the Bragg frequency, and L is the grating length. The stopband of the FBG is in the detuning range $-\kappa < \delta < \kappa$. The phase of the reflection is given by

$$\phi = \tan^{-1}\left[\frac{\alpha}{\delta}\frac{1}{\tanh h(\alpha L)}\right], \quad \alpha = \sqrt{\kappa^2 - \delta^2}. \tag{10}$$

To get the dispersion, we take the second derivative of the phase with respect to the frequency ω (using $d/d\omega = (n/c)d/d\delta$). We note that to make a strong grating κL must be much larger than 1 (typically $\kappa L \sim 10$), in which case $\operatorname{sech}(\kappa L) \approx 0$ and $\tanh(\kappa L) \approx 1$. The resulting dispersion may be expanded in a Taylor series around $\omega = \omega_B$ ($\delta = 0$) and keeping only the linear term in ω we get

$$\frac{d^2\phi}{d\omega^2} = \left(\frac{n}{c}\right)^2 \frac{d^2\phi}{d\delta^2} \approx \left(\frac{n}{c}\right)^2 \frac{\delta}{\kappa^3} = \left(\frac{n}{c}\right)^3 \frac{(\omega - \omega_B)}{\kappa^3}. \tag{11}$$

The region of low dispersion is where $(d^2\phi/d\omega^2)(\Delta\omega)^2 \ll 1$ and $\Delta\omega = 2(\omega - \omega_B)$ is the full bandwidth. The frequency range over which the dispersion is small is therefore given by

$$\Delta\omega \ll \frac{c\kappa}{n} \tag{12}$$

so the region for low dispersion is given by a bandwidth which is smaller than about the stopband, as we would expect.

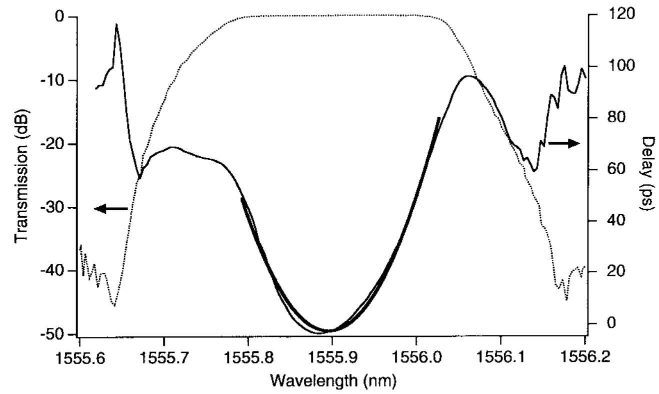

Fig. 7. Reflection spectrum (dotted line) and corresponding group delay (thin solid line) of an apodized FBG. The thick solid line is a quadratic fit to the group delay, indicating a dispersion linear in detuning in agreement with (11).

From the above equations we can see that for stronger gratings (larger κ, but still $L > 3/\kappa$) the dispersion slope will become smaller and the region of low dispersion will become larger. This is expected for MPF's since increasing κ makes the amplitude response wider, squarer, and flatter on top and flat regions in amplitude correspond to linear phase regions (as can be verified using (4); see also [14]). To get an idea of the effects of this kind of dispersion, we will evaluate the dispersion close to the band edge $\delta = 0.9\kappa$, using (11) we get a dispersion of $\sim 2100/\kappa^2$ in ps^2 where κ is in cm^{-1}. If we take $\kappa = 10$ cm^{-1} (and $L > 3$ mm), the resulting dispersion is 21 ps^2, which means that a Gaussian pulse of full width at half-maximum (FWHM) intensity of ~7.5 ps will broaden by a factor of $\sqrt{2}$ upon reflection off this grating [26]. This means that the usable fraction of the FBG's passband may be limited by the phase response (dispersion) rather than the amplitude response (flatness of the passband). Fig. 7 shows the measured reflection spectrum and corresponding group delay in reflection of an apodized grating. As can be seen, the delay in the center of the stopband can be fit very well with a quadratic, indicating that the dispersion is indeed linear over most of the passband in agreement with (11). A similar analysis was carried out for the dispersion experienced by the *transmitted* neighboring channel in [8] and will not be repeated here.

IV. Approximating the Ideal Rectangular Linear Phase Filter

The ideal filter of (1) is not a causal filter so it may only be approximated. The ideal filter is desirable since it would let us achieve the highest bandwidth utilization without coding; the channel bandwidth would be equal to the channel spacing and the spectral efficiency would be 1 bit/s/Hz. As we have pointed out, a MPF is not a good choice for approximating this ideal characteristic, since squaring the amplitude response comes at

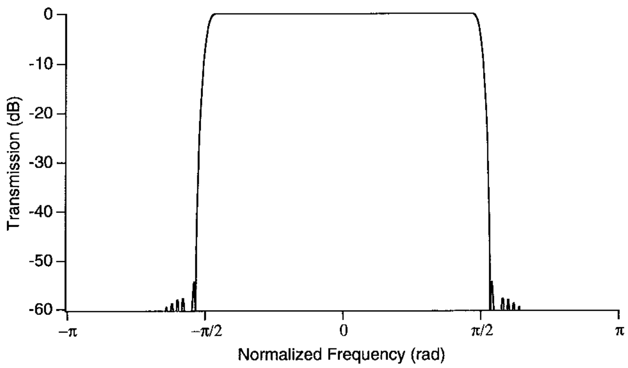

Fig. 8. Transmission spectrum of a digital filter with 101 delays using a Hamming window to achieve a very "square" response without affecting the linear phase properties of the filter. Even though this filter has extremely "sharp corners," it is dispersionless over the whole passband.

the price of nonlinear phase response. We would therefore like to adjust the phase response independently of the amplitude response and this is only possible with a non-MPF. In this case, we may take an existing "good" amplitude response and try to linearize the phase response over most of the passband. Two possible approaches are detailed below.

A. Using Class I Filters (WGR and MZI Based Filters)

As was shown, these filters are inherently suitable for linear phase filters. Using digital processing techniques such as windowing, the amplitude response may be made very rectangular without affecting the linear phase (by ensuring that $h(n)$ is symmetric). An example of this is given in Fig. 8 where a very sharp filter was designed such that $h(n)$ is the product of a truncated $\sin(x)/x$ function and a Hamming window [20]. Such a design may be hard to achieve practically since it requires a large number of delays N (101 in this example) and also a specifically tailored distribution of weights $h(n)$, some of which are negative and so would require a π phase shift. This indicates that a better approximation of the ideal filter comes at the price of added complexity. Note that the filter shown in this figure contains many zeros well outside the unit circle and is therefore non-MPF even when a little loss is added. There have recently been other practical approaches for flattening the passband [27], [28] which can be shown to still maintain their linear phase characteristics.

B. Using Class II or III Filters (Interference and FBG Type Filters)

As was pointed out earlier, these filters inherently contain poles, which destroy the linear phase characteristic. A standard technique in the design of electronic filters involves cascading an all-pass filter in series with the original filter. An all-pass filter does not modify the amplitude response but can correct the phase response (see Appendix D). An example of an optical all-pass filter is the Gires–Tournois interferometer mentioned earlier. Note that since by definition an all-pass filter is a non-MPF it would have to be a reflective filter. Using numerical optimization routines and commercial software for TFF design may yield the desirable all-pass filter design to correct the phase of a class II or class III filter. This design may not be manufacturable as a FBG if the required index modulation function is an aperiodic function. On the other hand, if the design requires many thin-film layers it may not be a practical class II filter. We have recently shown that an all-pass ring resonator filter may be designed for phase correction and yielding a corresponding increase in usable filter bandwidth [29]. Ultimately there will always be a tradeoff between amplitude response and phase response to get the highest possible bandwidth utilization with a reasonable filter complexity.

V. Conclusions

In this paper we have considered the phase response of various optical filters and their impact on WDM systems. This dispersion arises from structural or geometrical properties in contrast to material characteristics. The filters considered here are all based on interference of some sort, whether from different waveguides or from multiple reflections, whereas material dispersion arises from absorption peaks. These absorption peaks are always well-behaved functions and Kramers–Krönig relations always apply for the calculation of material dispersion. Structural dispersion may be zero because optical filters may be constructed such that they are non-MPF's in which case the Hilbert transform may not be used to infer the phase from the amplitude. This leads to the somewhat nonintuitive result that the phase response may be adjusted without affecting the amplitude result. In this way we gain an added degree of freedom toward the approximation of the ideal filter given by (1).

The optical filters considered in this paper are the most common ones considered in connection with WDM systems. These filters have response functions, which are identical to those of digital filters [(5) and (8)]. There is a fundamental difference between class I filters and class II and III filters. Class I filters are FIR filters that have only zeros and contain no inherent feedback mechanism, such as reflection, associated with them. Class II and III filters are IIR filters and have both poles and zeros and rely on a feedback mechanism namely reflection. Because FIR filters have no poles they are ideal candidates for linear phase filters. IIR filters, on the other hand, have poles that tend to distort the phase response.

Linear phase FIR filters may be designed which are arbitrarily close to the ideal filter in terms of the rectangular amplitude response. Even when there is some small loss introduced into these filters, the phase departs from linearity only very close to the passband edge where the attenuation is high. This performance comes at a price of increased filter complexity. In contrast, IIR filters inherently have a nonlinear phase response, which may be corrected over some bandwidth by cascading an all-pass filter in series (which may also come at a price of increased complexity). Class II and III *transmission* filters are always MPF's, so that once the amplitude response in transmission is known or measured the phase response may be calculated by means of a Hilbert transform. In this case, the phase response may be inferred almost by inspection of the amplitude response. This is due to the fact that for MPF's, broadly speaking, the phase follows the derivative of the amplitude response with the result that the "squaring" of the response leads to an increase in dispersion. Non-minimum phase all-pass filters, therefore, may only be achieved by utilizing a class II or III filter in *reflection*. The design and production of an all-pass filter that corrects the phase of a given class II or III filter may not be a trivial matter.

Once the dispersion is given, we can determine the effective bandwidth where the dispersion-induced pulse broadening does not lead to penalties and degradation in system performance. This effective bandwidth may be narrower than the bandwidth over which the amplitude response is flat. Similarly, when considering dispersion effects on neighboring channels, dispersion may dictate minimum channel spacing rather than crosstalk. Both effects lead to a waste in bandwidth and degradation in spectral efficiency. Thus the design of linear phase filters may become very important in future high aggregate bit rate systems.

APPENDIXES

In the following sections, we deal with some of the more technical and mathematical details of optical filter dispersion. We use standard digital signal terminology, which can be found in basic textbooks on digital signal processing [see e.g., 20].

APPENDIX A
LINEAR PHASE FIR FILTERS

In this appendix we discuss FIR filters and specifically FIR filters which have the property of having linear phase at all frequencies. FIR filters have a system function and frequency response of the form

$$H(z) = \sum_{n=0}^{N-1} h(n) z^{-n}$$
$$H(e^{j\omega}) = \sum_{n=0}^{N-1} h(n) e^{-j\omega n} \tag{A1}$$

and since $H(z)$ has no denominator polynomial, these filters have no poles and have only zeros. This reflects the fact that they are derived from a difference equation which can be written as

$$y(n) = \sum_{k=0}^{N-1} b_k x(n-k). \tag{A2}$$

We now examine the conditions under which the FIR filters are also linear phase filters. We first note that the second equation (A1) is the Fourier transform of $h(n)$ (since $h(n)$ is zero for $n<0$ and $n>N-1$ the limits in (A1) may be extended to $+\infty$). If $h(n)$ is even (symmetric), $h(n)=h(-n)$, and real, then its Fourier transform is a real and even function. In our case, $h(n)$ must be causal, but if it is even about its center (i.e., about $n = N/2$) it is a shifted symmetric function. A shift in $h(n)$ corresponds to a linear phase shift in the frequency domain and so this shifted function has a transform which is a real even function multiplied by a linear phase function. For the shifted $h(n)$ to be even, the condition $h(n) = h(N-1-n)$ must hold and this is the linear phase condition. As an example, we assume N even

$$\begin{aligned} H(e^{j\omega}) &= \sum_{n-0}^{N/2-1} h(n)e^{-j\omega n} + \sum_{n=N/2}^{N-1} h(n) e^{-j\omega n} \\ &= \sum_{n=0}^{N/2-1} h(n)e^{-j\omega n} + \sum_{n=0}^{N/2-1} h(N-1-n) \\ &\quad \cdot e^{-j\omega(N-1-n)} \\ &= \sum_{n=0}^{N/2-1} h(n)(e^{-j\omega n} + e^{-j\omega(N-1-n)}) \\ &= e^{-j\omega[(N-1)/2]} \sum_{n=0}^{N/2-1} 2h(n) \\ &\quad \cdot \cos\left[\omega\left(n - \frac{N-1}{2}\right)\right]. \end{aligned} \tag{A3}$$

This analysis is easily extended to odd N (and to antisymmetric $h(n)$ with N even). Another consequence of the symmetry of $h(n)$ is the location of the zeros of the system function $H(z)$, in the complex z plane. It can be shown [20] that the zeros may be on the unit circle at $z=\pm 1$ or in conjugate pairs (e.g., z_1 and z_1^*). Zeros that are not on the unit circle come in groups of four ($z_1, z_1^*, 1/z_1$, and $1/z_1^*$). In all of the above cases there are never zeros *inside* the unit circle and therefore linear phase filters are inherently non-MP. In Appendix B we will show that the above arrangement of zeros yields a constant group delay confirming the linear phase behavior of filters with zeros located as above.

The most trivial example of a linear phase filter is one where $h(n)$ is constant. The corresponding optical filter is a multiple-arm MZI where the relative phase shift between neighboring arms is constant. This optical filter is an idealized WGR and has linear phase everywhere and therefore no dispersion.

APPENDIX B
GROUP DELAY OF $H(z)$

In this appendix we discuss the general form of the group delay associated with a given frequency response. In all cases considered in this paper, the system function $H(z)$ is a rational function and may be written as the ratio of two polynomials in z

$$H(z) = \frac{\prod_{i=1}^{N}(z-z_i)}{\prod_{l=1}^{M}(z-z_l)} \tag{B1}$$

where the z_i and the z_l are the zeros and poles, respectively, and may be written in polar form as $z_k = \alpha_k e^{j\theta_k}$. To simplify, we have dropped all zeros and poles at $z=0$ (i.e., in (B1) we have dropped a prefactor of the form z^k), which corresponds to a linear phase factor in the following equation. Consequently, the expressions for group delay are given up to a constant group delay, which will have no contribution to the dispersion.

Replacing z with $e^{j\omega}$ we can now write the frequency response as follows:

$$H(e^{j\omega}) = \frac{\prod_{i=1}^{N}(e^{j\omega} - \alpha_i e^{j\theta_k})}{\prod_{l=1}^{M}(e^{j\omega} - \alpha_l e^{j\theta_l})} = \frac{\prod_{i=1}^{N}|e^{j\omega} - \alpha_i e^{j\theta_k}|}{\prod_{l=1}^{M}|e^{j\omega} - \alpha_l e^{j\theta_l}|} \exp[j\Phi(\omega)] \quad \text{(B2)}$$

where $\Phi(\omega)$ is the sum of the phases of all of the factors in the numerator and denominator, each factor having the form $\angle[\exp(j\omega) - \alpha\exp(j\theta)]$. Here the symbol $\angle$ indicates the phase angle or argument function. To get the phase we take the natural logarithm of the above frequency response and get

$$\Phi(\omega) = \sum_{i=1}^{N} \angle(e^{j\omega} - \alpha_i e^{j\theta_i}) - \sum_{l=1}^{M} \angle(e^{j\omega} - \alpha_l e^{j\theta_l}) \quad \text{(B3)}$$

Clearly, it is enough to look at one such factor and examine its contribution to the phase.

$$\phi(\omega) = \angle(e^{j\omega} - \alpha e^{j\theta}) = \tan^{-1}\left[\frac{\sin\omega - \alpha\sin\theta}{\cos\omega - \alpha\cos\theta}\right]. \quad \text{(B4)}$$

The group delay associated with one such factor is given by

$$\tau_g(\omega) = -\frac{d\phi(\omega)}{d\omega} = \frac{\alpha\cos\delta - 1}{(1+\alpha^2) - 2\alpha\cos\delta} \quad \text{(B5)}$$

where $\delta = \omega - \theta$. On the unit circle $\alpha = 1$ and $\tau_g(\omega) = -1/2$. We also note the following interesting property of the above function:

$$\tau_g(\delta, 1/\alpha) = -(1 + \tau_g(\delta, \alpha)). \quad \text{(B6)}$$

Fig. 9 shows the time delay as a function of δ for different values of $\alpha < 1$ [(B6) may be used for $\alpha > 1$] and the associated power transmission. As can be seen, when the unit circle is approached the delay becomes very peaked near $\omega = \theta$ and the transmission approaches zero.

If we have a pair of zeros located at z_1 and $1/z_1^*$ (i.e., at $\alpha e^{j\theta}$ and $(1/\alpha)e^{j\theta}$), the sum of their group delays will be a constant $\tau_g(\omega) = -1$. This is exactly how the zeros are located in a linear phase filter (see Appendix A); additional zeros on the unit circle contribute a constant delay too (as shown earlier). If the system function contains *only* zeros in this way, the total delay is a constant, the phase is linear, and the dispersion is zero.

IX. Appendix C
Digital Filter Representation of Multilayered Structures

In this appendix we discuss and derive some of the properties associated with class II and III filters when using a digital filter description. The representation of multilayered optical filters has been discussed in detail in [22]. In this appendix we repeat and emphasize some of the salient features that have bearing on the issues presented in this paper. This approach is based on computing the exact fields in each layer and relating the fields in consecutive layers through 2×2 transfer matrices of the form [22]

$$\frac{z^{1/2}}{t_k}\begin{pmatrix} z^{-1} & -r_k \\ -r_k z^{-1} & 1 \end{pmatrix}. \quad \text{(C1)}$$

This matrix connects the layer k and layer $k+1$, where r_k and t_k are the field reflection and transmission between the layers, respectively. z is the normal complex variable that eventually is evaluated at $z = e^{j\omega}$ to get the frequency response. In the above, the assumption is that all the layers have the same optical thickness (this is easily extended to the more general case, as shown in [22]). The only different matrix is the one for $k = 0$ where z is set to 1 in (C1). These matrices are now multiplied to relate the input and output fields. The total transfer matrix may be written as

$$\frac{z^{k/2}}{t_k \cdots t_0}\begin{pmatrix} A_k^R(z) & B_k^R(z) \\ B_k(z) & A_k(z) \end{pmatrix} \quad \text{(C2)}$$

and relates the fields between the input and output (with k interfaces in between). The polynomials with the R superscript are known as the reverse polynomials and, in the case of real coefficients (which is the case discussed here), are related to the forward polynomials through

$$A_k^R(z) = z^{-k}A_k(z^{-1}). \quad \text{(C3)}$$

This has the effect of exchanging first and last coefficients, second and second-to-last coefficients, etc. It can also be shown that the reverse polynomial has zeros which are conjugate symmetric to the zeros of the forward polynomial (i.e., if $A_k(z)$ has zeros at z_i then $A_k^R(z)$ has zeros at $1/z_i^*$). The

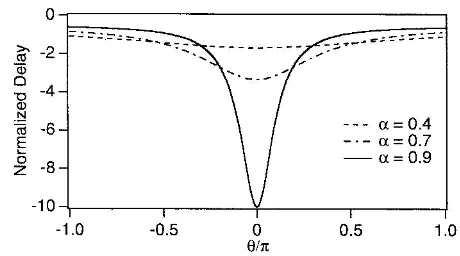

(a)

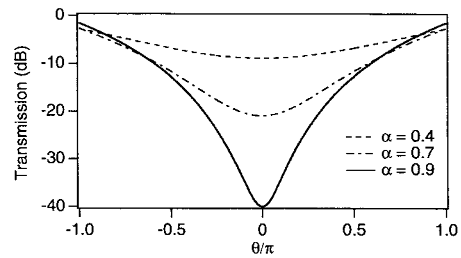

(b)

Fig. 9. (a) The group delay and (b) transmission associated with one zero of the system function located at $z = \alpha e^{j\theta}$, for different values of α.

reflection and transmission are now given by [22]

$$T(z) = \frac{z^{-k/2}(t_k \cdots t_0)}{A_k(z)}$$
$$R_L(z) = -\frac{B_k(z)}{A_k(z)}. \tag{C4}$$

Here the subscript L on the reflection refers to looking at the reflection from the "left side." In order to look at the reflection from the "right side" we need to make two changes: 1) change the sign on all the r_k's (since we are crossing all the interfaces in the opposite direction) and 2) multiply all the matrices in reverse. The total resulting matrix turns into

$$\begin{pmatrix} A_k^R(z) & -B_k(z) \\ -B_k^R(z) & A_k(z) \end{pmatrix} \tag{C5}$$

where the prefactor has been dropped since it does not affect the reflection which is now given by

$$R_R(z) = \frac{B_k^R(z)}{A_k(z)}. \tag{C6}$$

We can now make the following observations.

1) As can be seen from (C3), the transmission has no polynomial in the numerator and therefore no zeros. This implies that the transmission response is MP and there is a Hilbert transform relation between the amplitude and phase.
2) All the responses associated with the same structure $(T, R_L,$ and $R_R)$ have the same polynomial in the denominator.
3) Since the reverse polynomial has the conjugate symmetric zeroes of the forward polynomial, then if the reflection R_L is MP (all the zeros inside the unit circle) the reflection R_R is maximum phase (all the zeros outside the unit circle).
4) When the structure is symmetric, R_R and R_L are identical so that $B_k(z) = -B_k^R(z)$ which means that the numerator polynomial coefficients are symmetric (i.e., first and last coefficients are equal, etc.).

Next, we examine what can be said, in general, about the group delay. As was shown in Appendix B, the total group delay is the sum of the delays associated with each of the poles minus the sum of the delays associated with each of the zeros. From (C4) and (C6) we see that all three responses have the same contribution to the total group delay determined by the poles (roots of A_k), which we will call τ_{gp}. The total group delay contribution from the zeros of the forward polynomial (roots of B_k) will be written as τ_{gz}. Using this notation, the total delay in R_L is simply $\tau_{gp} - \tau_{gz}$. In Appendix B it was also pointed out that there is a simple relation (B6) between the delays of conjugate symmetric pairs. We use this fact to compute the delay of R_R and get $\tau_{gp} + \tau_{gz} + \tau_c$, where τ_c is a constant (frequency-independent) group delay. This constant group delay is related to the choice of reference planes: the reference plane for R_R is at $x = L$ but the reference plane for R_L is at $x = 0$ and τ_c is a measure of the transit time through the structure length L [24], [25]. From the above we see that the sum of the delays in reflection (from R_L and R_R) is equal to twice the delay in transmission [note that the delay in transmission *also* includes a constant delay arising from the $z^{-k/2}$ term in $T(z)$ in (C3)]. This relation was also pointed out in [24].

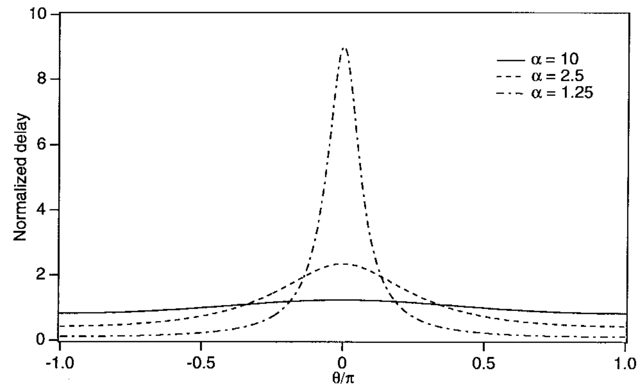

Fig. 10. The group delay associated with a single-stage all-pass filter with a zero located at $z = \alpha e^{j\theta}$ and a pole located at $z = (1/\alpha)e^{j\theta}$, for different values of α.

Finally, if the structure is symmetric then the time delays in R_L and R_R must be equal, implying that τ_{gz} is a constant. As was pointed out in Section III-B, a symmetric structure may be non-MP, however, if the constant group delay is removed, the remaining delay is due only to the poles, in which case we are back to an MP situation. Note also that since τ_c is constant in frequency it does not contribute to the dispersion.

APPENDIX D
ALL-PASS FILTERS

In this appendix we discuss all-pass filters and their phase correcting properties. All-pass filters have constant amplitude response over all frequencies and are therefore well suited for phase equalization—the phase may be tailored without adjusting the amplitude. This immediately implies that all-pass filters are non-MP. All-pass filters have the following system function $H(z)$:

$$H(z) = \frac{\prod_{i=1}^{N}(z - z_i)}{\prod_{i=1}^{N}(z - 1/z_i^*)}. \tag{D1}$$

This means that the zeros and poles come as conjugate symmetric pairs. Here, as in Appendix B, we ignore the zeros and poles at $z = 0$, which do not contribute to the dispersion. To understand this filter better we look at one such pair in the frequency response with a zero at $z_i = \alpha e^{j\theta}$ and a pole at $(1/\alpha)e^{j\theta}$:

$$H(e^{j\omega}) = \frac{e^{j\omega} - \alpha e^{j\theta}}{e^{j\omega} - (1/\alpha)e^{j\theta}}. \tag{D2}$$

It can be easily verified that this frequency response has a frequency-independent amplitude response. The corresponding group delay of this single-stage all-pass filter is

$$\tau_g = \frac{-1 + \alpha^2}{1 + \alpha^2 - 2\alpha\cos\delta}. \tag{D3}$$

Fig. 10 shows this group delay for different values of α (with $\alpha > 1$ so that the poles lie inside the unit circle). Here again the delay is sharply peaked near $\omega = \theta$ and diverges as the unit circle $\alpha = 1$ is approached), but the amplitude response is *flat*. By building up a multistage all-pass filter (which is just a product of many single-stage all-pass filters), the group delay may be adjusted at many frequencies. This may become very complex and require many all-pass stages if the phase response is complicated.

Acknowledgment

The authors would like to thank C. Doerr, C. Dragone, C. H. Henry, W. H. Knox, H. Kogelnik, M. Margalit, and L. E. Nelson for many enlightening discussions on this subject.

References

[1] C. Dragone, "An $N \times N$ optical multiplexer using a planar arrangement of two star couplers," *IEEE Photon. Technol. Lett.*, vol. 3, pp. 812–815, 1991.
[2] Y. P. Li, C. H. Henry, E. J. Laskowski, and H. H. Yaffe, "Fourier transform based optical waveguide filters and WDM's," in *OFC'96 Tech. Dig.*, vol. 2, pp. 97–98, 1996.
[3] M. A. Scobey and D. E. Spock, "Passive DWDM components using MicroPlasma® optical interference filters," in *OFC'96 Tech. Dig.*, vol. 2, pp. 242–243, 1996.
[4] C. Madsen and J. Zhao, "A general planar waveguide autoregressive optical filter," *J. Lightwave Technol.*, vol. 14, pp. 437–447, 1996.
[5] T. A. Strasser, P. J. Chandonnet, J. DeMarko, C. E. Soccolich, J. R. Pedrazzani, D. J. DiGiovanni, M. J. Andrejco, and D. S. Shenk, "UV-induced fiber grating OADM devices for efficient bandwidth utilization," in *OFC'96*, postdeadline paper PD8.
[6] M. C. Farries, K. Sugden, D. C. J. Reid, I. Bennion, A. Molony, and M. J. Goodwin, "Very broad reflection bandwidth (44 nm) chirped fiber gratings and narrow bandpass filters produced by the use of an amplitude mask," *Electron. Lett.*, vol. 30, pp. 891–892, 1994.
[7] C. Latrasse, M. Breton, M. Têtu, N. Cyr, R. Roberge, and B. Villeneuve, "C_2HD and $^{13}C_2H_2$ absorption lines near 1530 nm for semiconductor-laser frequency locking," *Opt. Lett.*, vol. 19, pp. 1885–1887, 1994.
[8] B. J. Eggleton, G. Lenz, N. Litchinitser, D. B. Patterson, and R. E. Slusher, "Implications of fiber grating dispersion for WDM communication systems," *IEEE Photon. Technol. Lett.*, vol. 9, pp. 1403–1405, 1997.
[9] G. Lenz, B. J. Eggleton, C. K. Madsen, C. R. Giles, and G. Nykolak, "Optimal dispersion of optical filters for WDM systems," *IEEE Photon. Technol. Lett.*, vol. 10, pp. 567–569, 1998.
[10] A. H. Gnauck and R. M. Jopson, "Dispersion compensation for optical fiber systems," in *Optical Fiber Telecommunication IIIA*, I. P. Kaminow and T. L. Koch, Eds. San Diego, CA: Academic, 1997.
[11] M. Beck, I. A. Walmsley, and J. D. Kafka, "Group delay measurements of optical components near 800 nm," *IEEE J. Quantum Electron.*, vol. 27, pp. 2074–2081, 1991.
[12] H. M. Nussenzveig, *Causality and Dispersion Relations*. New York: Academic, 1972.
[13] D. C. Hutchings, M. Sheik-Bahae, D. J. Hagan, and E. W. Van Stryland, "Kramers–Krönig relations in nonlinear optics," *Opt. Quantum Electron.*, vol. 24, pp. 1–30, 1992.
[14] H. W. Bode, *Network Analysis and Feedback Amplifier Design*. New York: Van Nostrand Company, 1945.
[15] D. Marcuse, *Theory of Dielectric Optical Waveguides*, 2nd ed. San Diego, CA: Academic, 1991.
[16] O. E. Martinez, "Matrix formlism for pulse compressors," *IEEE J. Quantum Electron.*, vol. 24, pp. 2530–2536, 1988.
[17] R. H. J. Kop, P. de Vries, R. Sprik, and A. Lagendijk, "Kramers-Kronig relations for an interferometer," *Opt. Commun.*, vol. 138, pp. 118–126, 1997.
[18] N. Balabanian and W. R. LePage, "What is a minimum-phase network?" *Trans. Amer. Inst. Elect. Eng.*, vol. 75, pp. 785–788, 1956.
[19] Y. Sun, J. W. Sulhoff, A. K. Srivastava, J. L. Zyskind, C. Wolf, T. A. Strasser, J. R. Pedrazzani, J. B. Judkins, R. P. Espindola, A. M. Vengsarkar, and J. Zhuo, "Ultra wide band Erbium-doped silica fiber amplifier with 80 nm of bandwidth," in *Optical Amplifiers and their Applications Conf.*, Victoria, BC, Canada, July 21–23, 1997, post deadline paper PD2.
[20] A. V. Oppenheim and R. W. Schafer, *Digital Signal Processing*. Englewood Cliffs, NJ: Prentice-Hall, 1975.
[21] P. Yeh, *Optical Waves in Layered Media*. New York: Wiley, 1988.
[22] E. M. Dowling and D. L. MacFarlane, "Lightwave lattice filters for optically multiplexed communication systems," *J. Lightwave Technol.*, vol. 12, pp. 471–486, 1994.
[23] A. Carballar and M. A. Muriel, "Phase reconstruction from reflectivity in fiber Bragg gratings," *J. Lightwave. Technol.*, vol. 15, pp. 1314–1322, 1997.
[24] L. Poladian, "Group-delay reconstruction for fiber Bragg gratings in reflection and transmission," *Opt. Lett.*, vol. 22, pp. 1571–1573, 1997.
[25] E. Brinkmeyer, "Simple algorithm for reconstructing fiber gratings from reflectometric data," *Opt. Lett.*, vol. 20, pp. 810–812, 1995.
[26] G. P. Agrawal, *Nonlinear Fiber Optics*. San Diego, CA: Academic, 1989.
[27] C. Dragone, T. Strasser, G. A. Bogert, L. W. Stulz, and P. Chou, "Waveguide grating router with maximally flat passband produced by spatial filtering," *Electron. Lett.*, vol. 33, pp. 1312–1314, 1997.
[28] C. Dragone, "Frequency routing device having a wide and substantially flat pass-band," U.S. patent 5412744, May 2, 1995.
[29] C. K. Madsen and G. Lenz, "Optical all-pass filters for phase response design with applications for dispersion compensation," *IEEE Photon. Technol. Lett.*, vol. 10, pp. 994–996, July 1998.

G. Lenz, photograph and biography not available at the time of publication.

B. J. Eggleton, photograph and biography not available at the time of publication.

C. R. Giles, photograph and biography not available at the time of publication.

C. K. Madsen, photograph and biography not available at the time of publication.

R. E. Slusher, photograph and biography not available at the time of publication.